IEEE Access
Multidisciplinary | Rapid Review | Open Access Journal

Received 6 February 2024, accepted 11 March 2024, date of publication 20 March 2024, date of current version 27 March 2024.

Digital Object Identifier 10.1109/ACCESS.2024.3379737

RESEARCH ARTICLE

Advanced Control Architectures for Quantum Satellite Temporal-Networking

FRANCESCO CHITI, (Senior Member, IEEE), ROBERTO PICCHI, (Member, IEEE), AND LAURA PIERUCCI, (Senior Member, IEEE)
Department of Information Engineering, University of Florence, 50139 Florence, Italy
Corresponding author: Roberto Picchi (roberto.picchi@unifi.it)

ABSTRACT The use of quantum satellites can be significant paving the way for novel telecommunications network paradigms, making it possible to connect remote regions. Given the rapid development of quantum communication technologies, many studies are focusing on quantum satellites interconnections via Free Space Optic (FSO), especially considering that the adoption of wired alternatives did not achieve significant results, mainly in terms of covering long distances. In this context, the global interconnection of Quantum Computers (QCs) through the so-called Quantum Internet (QI) compels for new communications and computing architectures such as Quantum Cloud (QCloud). To this purpose, the deployment of Satellite Quantum Networks (SQNs) could make easily available innovative services spanning from security to advanced computing, especially by using Software-Defined Networking (SDN) technology, which is considered a significant enabler for the management of SQNs. Moreover, considering the rapid variability of the topology in terms of nodes and links features, the paper proposes a specific Temporal Networks (TNs) optimization strategy embedded in an SDN Controller ecosystem, dynamically optimizing the path durations to achieve the highest entanglement rate, while limiting the disconnections. Performance evaluation in a worst case scenario shows that the proposed framework is able to support distributed applications by exploiting all the connection opportunities.

INDEX TERMS Global quantum communication networks, quantum satellite systems, quantum software-defined networking, temporal networks.

I. INTRODUCTION

The design of new integrated telecommunications networks paradigms and technologies is made necessary by the significant growth of the number of heterogeneous devices and the development of innovative services [1]. In particular, satellite networks constitute a promising solution, considering that they allow connecting regions where it is not convenient to build a terrestrial infrastructure, thereby complementing the terrestrial segment of the 5G and 6G networks [2].

Recently, quantum technologies are emerging for creating new generation networks beyond the 6G [3], according to the quantum entanglement and teleportation [4], [5], but relaying on the use of satellite links [6], [7], [8]. Many of the services that Quantum Networks (QNs) will enable are still open issues; however, it is likely that they are going to support distributed quantum computing systems [9].

Nevertheless, as described in [10], it is still very difficult to obtain entanglement on Optical Fibers (OFs), given their significant attenuation. Therefore it is necessary to rely on satellites acting as Quantum Repeaters (QRs) to increase the distance at which the entanglement can be obtained and minimize the number of involved devices. A dedicated protocol which requires several phases is used to create an intersatellite quantum path between two Ground Stations (GSs), which is defined as End-to-End (E2E) quantum connection [11]. Specifically, the operation of entanglement swapping is performed recursively on the Quantum Satellite

The associate editor coordinating the review of this manuscript and approving it for publication was Vittorio Camarchia.

Repeaters (QSRs) that compose the E2E path, i.e., multiple Bell states measurements [12] are executed on the nodes following a specific order [13], [14], [15].

A communication through a quantum satellite backbone have to be performed with the use of two specific links [16]:

- Inter-satellite links: the satellites in Line of Sight (LoS) can share entangled photons.
- Ground-to-Satellite (G2S) and Satellite-to-Ground (S2G) links: the entangled particles are shared between a GS and a satellite.

The G2S and the S2G links result particularly critical considering all the degradation effects introduced by the atmosphere. However, the generated entangled states can be preserved with higher fidelity than OFs [17].

It is necessary to consider that, especially in a Low Earth Orbit (LEO) satellite scenario, the links between single satellites and between satellites and GSs are time varying. For instance, given their high velocity, a GS remains in contact with a LEO satellite for a reduced time window [18]. Therefore, this kind of scenario can be studied applying the Temporal Network (TN) theory [19]. As a matter of fact, many real-world graphs can be represented as *temporal graphs*, in which the vertex are in contact during specific time windows, hence, affecting the E2E connectivity [20]. Temporal graphs were usually represented as multiple static graphs because they were considered much easier to handle [21]. However, even though calculating a set of subgraphs and performing multiple iterations of routing algorithm across them may seem like a feasible solution, it can be very computationally onerous as the number of satellites increases. Therefore, several strategies have been developed for managing TNs, such as the one considered in this paper, which is based on a unique integrated temporal graph, whose links are characterized by the average values of the weights defined in terms of Euclidean distance over time. Moreover, a specific routing algorithm has been proposed in the paper to find paths valid for long time intervals without the need for multiple iterations.

A paradigm that is considered crucial for the development of future QNs is Software-Defined Networking (SDN) [22]. In particular, SDN decouples the Control Plane (CP) from the Data Plane (DP), providing the use of a logically centralized Controller with a comprehensive view of the network, which controls multiple devices that can be configured via specific southbound interfaces, to satisfy the requirements of the Application Plane (AP) [23]. Taking into account that QNs need an abstraction of the hardware in order to specify the forwarding rules, the term Quantum SDN (QSDN) was defined. Specifically, in the Satellite Quantum Networks (SQNs) case, SDN allows to address all the typical challenges and to program the QSRs, which are the devices composing the DP, to operate properly only within specific time intervals [24]. The CP, which is designed to manage routing and signaling operations, is decoupled from the DP that is dedicated to the creation of Bell pairs. The CP traffic, constituted of routing and signaling messages is exchanged through a classical channel, while DP traffic, which is composed of Bell pairs, is sent over a dedicated quantum channel [6]. Furthermore, given the specific features of the devices that constitute the DP of QNs w.r.t. classical networks, it is necessary to provide the design of specific protocols and interfaces for the realization of a QSDN, to satisfy the requirements of the quantum AP, which includes distributed quantum computing and Quantum Key Distribution (QKD) services. In addition, given the previous considerations, the integration of a temporal graph with a properly designed optimization strategy in an SDN architecture is definitely a viable solution.

Therefore, this paper proposes an effective and innovative framework to design a quantum satellite backbone network, which is composed of satellites that operate as QRs with the contributions listed as follows:

- The definition of an architecture based on the SDN principle. In particular, the architecture provides the interaction between a Master Control Station (MCS) on the ground and an SDN Controller embedded in the QSR constellation.
- A novel optimization method for calculating E2E paths based on the TNs theory to maintain service continuity, ensuring the best possible performance in terms of entanglement rate during specific time intervals.
- A protocol specifically developed for the considered architecture that allows to coordinate the action of the elements that constitute the CP and manage the elements of the DP.

This manuscript is structured as follows: Section II provides a summary of the most recent related works. Section III discusses the system model. Specifically, Section III-A provides an overview of the architecture and the proposed path selection algorithm. Moreover, Section III-B describes the specifically designed protocol. Section IV describes the simulation environment, the system implementation, and validation. Finally, Section V outlines the conclusions and possible future perspectives.

II. RELATED WORKS

The main characteristic of QI is to be able to interconnect several QCs to obtain a significant computational capacity. The infrastructure that allows to realize the physical interconnection between two nodes has to be designed considering their distance.

As explained in [25], with the use of OFs, a large portion of the photons that compose the beam scatter before reaching the optical receiver, and the number of entanglements created per second decreases exponentially as the distance increases. Therefore, it is important to take into consideration several communication technologies, such as satellites [22], [26]

that can also interoperate with terrestrial scenarios as described in [27].

The Micius satellite, which operates in LEO, was used to distribute quantum keys between multiple GSs on a continental scale [28]. The distance between the satellite and a single GS varies from 500 to 1400 *km* during the transition. Furthermore, the qubits generated on the ground were teleported to the satellite [29].

In [30], the authors present an approach for global quantum networking using a space and a ground network segment. Specifically, the study provides an investigation of the achievable key rates for different QMs embedded into the devices used for the implementation of several QKD protocols. Furthermore, it also analyses the effects of the beam pointing errors and memory efficiencies on the performance of the analyzed QKD protocols. Moreover, in [31], several schemes that employ quantum satellites equipped with QMs for continental and intercontinental scenarios have been analyzed.

However, the use of satellite is only part of the solution. As a matter of fact, it is important to consider the use of SDN [22], [26] in order to control a quantum satellite backbone. Specifically, [6] presents a single SDN Controller architecture, with the SDN Controller located on the ground. In addition, the paper presents a performance analysis of several path selection algorithms, which are applied to multiple static graphs. Moreover, [7] proposes a comparable design, with a performance evaluation of various constellations, providing that LEO ensures better performance than Medium Earth Orbit (MEO) constellations. Nevertheless, the studies described previously regarding the use of a single Controller positioned on Earth. The first study that presents an architecture with multiple Controllers deployed in a quantum satellite constellation is [8]. In particular, the proposed architecture is composed of multiple SDN Controllers with different purposes, many of them integrated into the constellation and it operates hierarchically, as is done in some contexts regarding classical communications [32], [33]. A similar approach has been also used in [34]. Furthermore, a mobile CP solution with multiple Controllers is also presented in [35].

The studies on TNs are not recent, and some algorithms applicable on temporal graphs have been proposed in [21]. Moreover, as described in [19], the TN theory has been applied in several research areas, such as cell biology, ecological networks, air-transport networks, physical proximity, distributed computing and networks. However, to the best of our knowledge, this theory has not yet been applied to specific contexts, such as those related to satellite networks and, in particular, QSRs scenarios. Considering the rapid variation of the positions of LEO satellites, the TN theory may be particularly useful for the analysis and optimization of Satellite Quantum Networks (SQNs) as considered in this paper.

III. SYSTEM MODEL

This Section describes the proposed architecture considering the elements that constitute the CP and the DP. Furthermore, the proposed temporal path selection algorithm and a specifically designed protocol are also described.

A. ARCHITECTURE

The proposed architecture that is depicted in Fig. 1 is composed of MCS on the ground, which is the specific control node of the constellation typical of many other satellite systems such as the Global Positioning System (GPS) [36]. The MCS is connected with the GSs that in turn use a LEO satellite constellation to communicate. The CP architecture is based on the use of SDN paradigm, and the functional controller blocks that have been designed are the following:

1) Topology Manager (MCS)
2) Forwarding Manager (Satellite SDN Controller)

The Topology Manager can integrate specific TN algorithms. As a matter of fact, in a constellation, the satellites are in contact with each other and with the GSs at specific time intervals; therefore, it can be described as a time varying network [37] and can be represented by the MCS as a temporal graph [38]. In particular, a temporal graph can be expressed as $\Gamma = (\Phi, \Psi)$, where Φ is the set of vertices, which in our case are the satellites, and Ψ is the set of edges that model both the quantum and classical inter-satellite links [21]. An edge $\psi \in \Psi$ is composed of five parameters $(i, j, t_{start_{i,j}}, t_{end_{i,j}}, w_{i,j}(t))$, where $i, j \in \Phi$, $t_{start_{i,j}}$ and $t_{end_{i,j}}$ are the bounds of the time interval during which the link exists, while $w_{i,j}(t)$ is the generic weight associated to it that varies over the related time interval.

The objective function to be optimized is the entanglement rate [10], which is the number of transmitted entangled states per second and is measured as Bell pairs per second. To characterize this metric, we used the model defined in [6], in which the probability of success in order to generate entanglement between two adjacent nodes depends on the Euclidean distance between them, the characteristics of the medium and the efficiency of the devices. Specifically, the entanglement generation probability is defined as:

$$p_{i,j} = \frac{1}{2}\eta_0(p_g\eta_h\eta_d)^2 e^{-\frac{d_{i,j}}{L_\alpha}} \tag{1}$$

where η_0, η_h and η_d are respectively the optical efficiency, the heralding and the entangling detector efficiency, p_g is the photons generation probability, while $d_{i,j}$ is the Euclidean distance between the two nodes and L_α indicates the electric field attenuation length. Therefore, the weight associated with the edge that exists in a specific time interval $[t_{start_{i,j}}, t_{end_{i,j}}]$ is the average $d_{i,j}(t)$ between the nodes i and j over the considered time interval. In order to maximize the achievable entanglement rate it is important to maintain these distances as low as possible to minimize

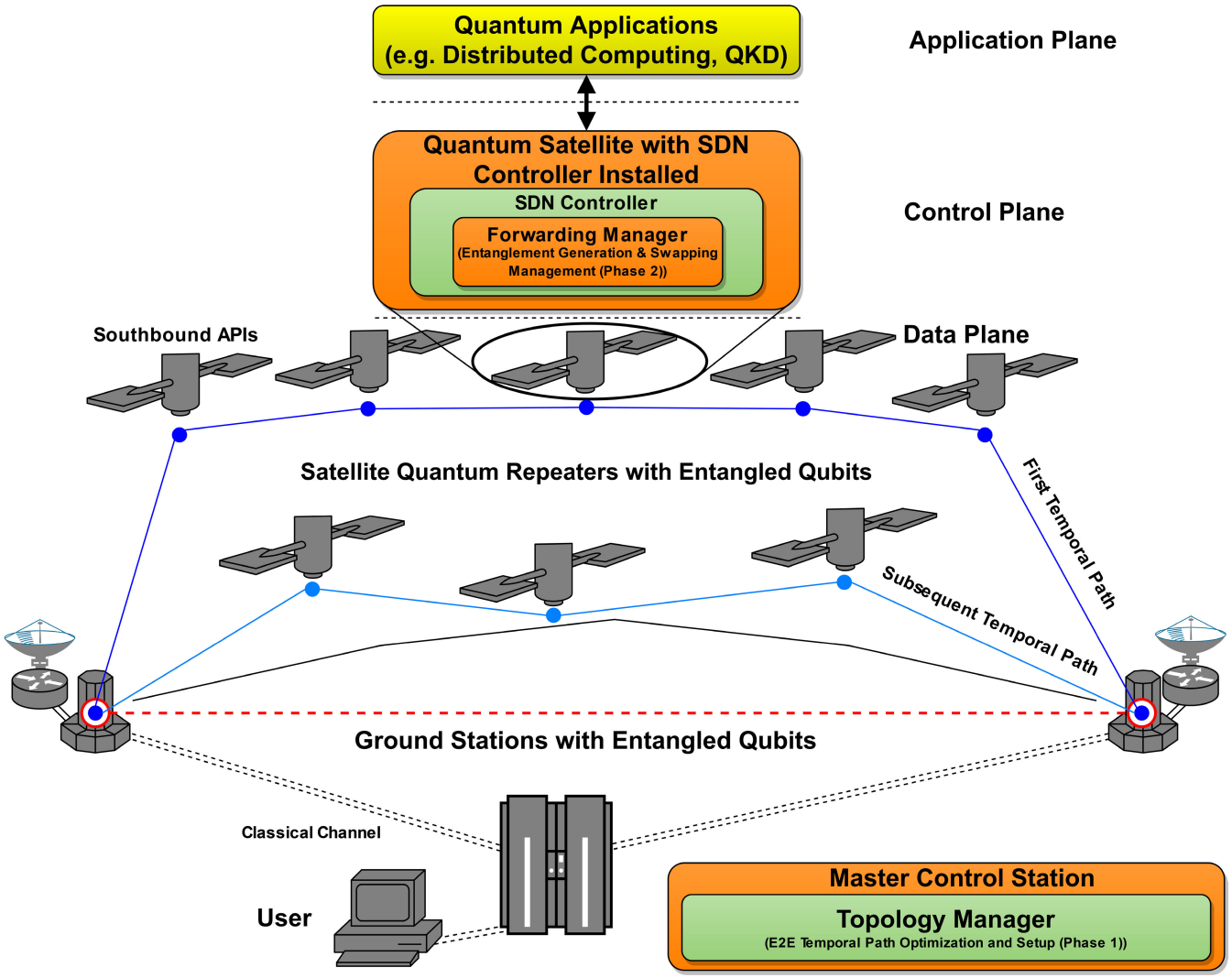

FIGURE 1. Quantum SDN satellite backbone. During phase 1, the optimal temporal E2E paths are calculated according to the results of the proposed optimization procedure, which is performed on the temporal graph. In the second phase, multiple Einstein-Podolsky-Rosen (EPR) pairs are created between the GSs through the operations programmed by the SDN Controller, which is enabled in a specific quantum satellite. Phase 2 is repeated every time the E2E path expires.

the latencies of classical signals. In particular, these are the classical bits of quantum teleportation operations related to the measurement operations of quantum states, and the signaling traffic related to ack transmission between the nodes over the classical communication link. Moreover, as expressed in [10], the entanglement rate also depends on second order parameters that characterize the QRs, such as the time required for the measurement operation, the time expectation for telecom-cavity and heralding-cavity output, the time required for cooling the memory cell before to start a new entanglement generation, and the duration of the pulse required to excite the memory cell [6], [10], [39], [40], [41], [42], which values are expressed in Table 1.

The optimization procedure then acts by minimizing the summation of the average costs of the single links that compose the path:

$$\begin{aligned} &\underset{W}{\text{argmin}} \sum_{i,j} \bar{w}_{i,j}(t) \\ &\text{s. t. } t_{start_{i,j}} \leq T_{start_{GS_{1,2}}} \\ &\qquad t_{end_{i,j}} \geq T_{end_{GS_{1,2}}} \\ &\qquad \forall \mathcal{L}_{i,j} \in P_{GS_1,GS_2} \subseteq \Psi \end{aligned} \tag{2}$$

where $W = (\bar{w}_{i,j})$ is the set of average weights assigned to each link, $T_{start_{GS_{1,2}}}$ and $T_{end_{GS_{1,2}}}$ are the time limits within which the GSs are simultaneously in contact with the respective satellites that are in LoS for the longest time intervals, $\mathcal{L}_{i,j}$ represents the link between two adjacent nodes and P_{GS_1,GS_2} is a subset of Ψ that includes the links composing the E2E paths. The transfer of entangled photons on the quantum channel and classical bits of the teleportation

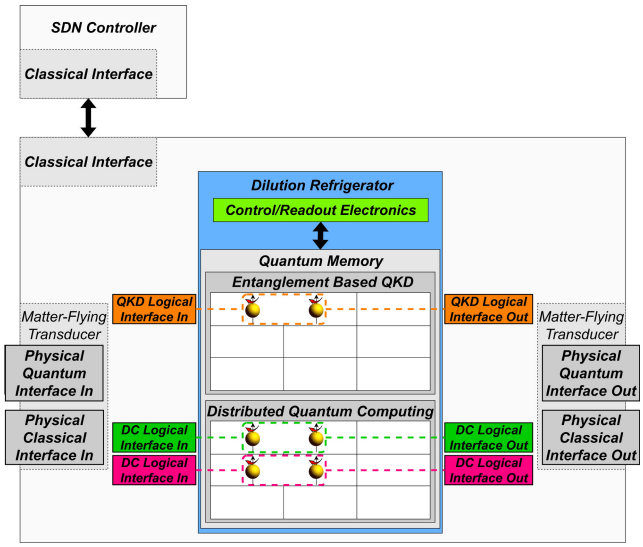

FIGURE 2. Possible architecture of a QR that can be installed on a satellite. Particles highlighted with the same color represent the pairs on which the swapping operation is performed.

process requires a time that is equal to the propagation delay, which is dominant, and the E2E delay is additive, with each addend given by the ratio $\frac{d_{i,j}(t)}{c}$ that is proportional to the distance and includes the speed of light c as denominator. Specifically, the optimization problem that we have developed minimizes the propagation delays operating on $d_{i,j}(t)$, and, therefore, the average weight are expressed as follows:

$$\bar{w}_{i,j}(t) \doteq \frac{1}{t_{end_{i,j}} - t_{start_{i,j}}} \int_{t_{start_{i,j}}}^{t_{end_{i,j}}} d_{i,j}(t)\, dt \tag{3}$$

Considering that, especially for LEO constellations, the time interval in which a GS is in visibility with the satellites in transit is limited to a few minutes, we considered to establish an E2E path between the satellites in visibility with the GSs for the longest time interval to guarantee the most durable entanglement generation sessions. Differently from the solution that we propose, the application of the Non-Temporal Dijkstra's algorithm to a temporal graph generates inconsistent solutions [43] that do not satisfy the temporal constraints and, therefore, do not generate valid E2E paths. Furthermore, the adopted optimization criteria was designed in order to limit the continuous disconnections between the GSs and the satellites in direct contact and make the connection as continuous as possible. In particular, the optimization methodology we proposed allows the creation of an E2E path with minimum weight in terms of distance and whose lifetime corresponds to the time interval in which GSs are simultaneously in contact with the respective satellites, whose transit time is the longest.

Given that many LEO orbits are Sun Synchronous Orbits (SSO) [44], also called a heliosynchronous orbit, the temporal graph could be calculated over 24 h and be valid for a long time unless possible trajectory corrections or faults occur. In the considered scenario, the GSs are not part of the temporal graph that pertains only to the satellite constellation. As a matter of fact, GSs could be mobile, and new users could be introduced making the overall temporal graph extremely complex and requiring frequent refreshing.

Considering that during this time window the satellites are surely in contact, it is possible to program the devices to work following a *proactive* approach [45].

Every time it is required to connect two GSs, the application invokes the MCS best path evaluation procedure. The QSRs, which are the devices that compose the DP, generate and exchange the Bell pairs taking into account the information provided by the SDN Controller via the southbound API. A representation of the elements that compose the device installed on board a satellite is shown in Fig. 2. Specifically, in addition to representing some of the typical elements of a QD, Fig. 2 represents the physical and logical interfaces.

To perform the E2E coupling procedure quickly and limit the traffic on the Ground-to-Satellite and Satellite-to-Ground links that can be perturbed by phenomena such as atmospheric turbulence [46], it is important to choose properly the satellite on which to enable the SDN Controller. In order to make the procedure as efficient as possible, the Controller is allocated on a satellite positioned in the middle of the path which sends to the other satellites in the path some specific control messages for the management of entanglement generation and swapping procedures. The creation of the EPR Pairs starts and proceeds towards both GSs. The entanglement generation procedure on the links that compose the E2E path can be accomplished according to the schemes described in [47] that require a coordinated action between the nodes at the two ends of the inter-satellite link and between the GSs and the connected satellite. Once the multiple Link-to-Link (L2L) connections via EPR pairs have been established, the swapping operations initiate, and the E2E entanglement is created. When the E2E path is no longer valid because the satellites that compose it are no longer in LoS, a new path is configured, and the procedure is reinitialized. The CP traffic needed to perform this procedure is all exchanged through the classic channel.

B. SESSION SET-UP

This Section describes the proposed protocol, which has been specifically conceived for the architecture represented in Fig. 1. The protocol is structured in two different phases:

1) Management of the connection requests between the GSs, optimal path calculation and SDN Controller placement.
2) Optimal path configuration performed by the SDN Controller.

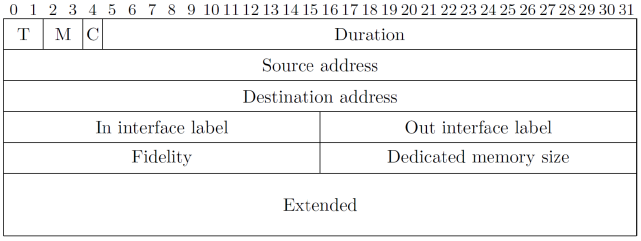

FIGURE 3. Packet format defined for the proposed protocol.

Furthermore, we have conceived a specific packet format with the aim to manage these operations properly. The packet is represented in Fig. 3, whose fields are below specified:

- `T`: this field defines the packet type and it is composed of 2 bits.
- `M`: it is composed of 2 bits and defines the entanglement generation and swapping modality.
- `C`: this field allows to enable the SDN Controller on a specific QSR and it is composed of a single bit.
- `Duration`: specifies the E2E path duration in milliseconds, which was previously calculated by the proposed temporal algorithm. Enables the satellites which are part of the E2E path to operate during a specific time interval, which can have a theoretical duration of 2^{27} *ms*.
- `Source address`: address of the source of the message.
- `Destination address`: address of the recipient of the message.
- `In interface label`: it is a field composed of 16 bits and specify the source port.
- `Out interface label`: as the previous field, it is composed of 16 bits, and it specifies the destination port.
- `Fidelity`: this field is reserved for future developments. For instance, it could contain the value of the requested fidelity. The considered model [6], [7], [10] neglects the effects of entanglement purification, considering that the adopted QR model is characterized by a very high fidelity, with values close to $F = 0.99$. However, the protocol provides the possibility to configure the path also according to the variation of other types of parameters.
- `Dedicated memory size`: this field is reserved for future developments. It contains the number of QSR memory qubits to be used for a specific session.
- `Extended`: it can contain the list of satellites composing the path with which the SDN Controller will need to interface in order to configure it.

A sequence diagram of the protocol is represented in Fig. 4 and it is described in the following. During the first phase, the connection request originated by one of the GSs is processed by the MCS that is positioned on the ground. The MCS receives a specific message with `T` configured as 0 and the `Source address` containing the IP address of the GS that requests the connection, and with the `Destination address` field containing the IP address of the other GS, with which it requires to establish a connection.

Therefore, the MCS starts to compute the E2E best paths for all the time intervals wherein the GSs are simultaneously in contact with the favorable satellites using the proposed algorithm and derivates a list.

In the proposed architecture that is represented in Fig. 1, the best E2E path is calculated by the MCS on the ground. Specifically, the MCS applies the proposed optimization procedure previously explained on the temporal graph. The pseudocode of the proposed algorithm is provided in Alg. 1. If N_s and N_d are respectively, the number of satellites in contact with the proxy satellites which in turn are in contact with the source GS and destination GS, and $\Theta(N^2)$ is the complexity of Dijkstra's algorithm, the complexity of Alg. 1 results $N_s N_d \Theta(N^2)$.

Algorithm 1 Best Temporal Path

Input: Temporal graph Γ
Output: List of best temporal paths L_{bp}
Initialization:
Calculate GSs most durable satellites tables *GS Source* (*GSS*) and *GS Destination* (*GSD*)
Merge *GSS* and *GSD* tables and create a unique table of simultaneously contact intervals *GS Contact* (*GSC*)
for each row in *GSC* **do**
  Get the S_s and S_d satellites in contact for each GS
  Get C_s and C_d satellite lists in contact with S_s and S_d
  for each satellite $\in$ C_s *and* C_d **do**
    Apply Dijkstra's algorithm and create a list of paths L_p
  end for
  Sort L_p in ascending $\sum \bar{w}_{i,j}(t)$ order
  for each path $P_k \in L_p$ **do**
    for each edge $\psi_{i,j} \in L_p$ **do**
      if $(t_{start_{i,j}} \leq T_{start_{GS_{1,2}}} \wedge t_{end_{i,j}} \geq T_{end_{GS_{1,2}}})$ **then**
        Declare $\psi_{i,j}$ available
      else
        Declare P_k unavailable
        break
      end if
    end for
    if P_k available **then**
      Add P_k to L_{bp}
      break
    end if
  end for
end for
return L_{bp}

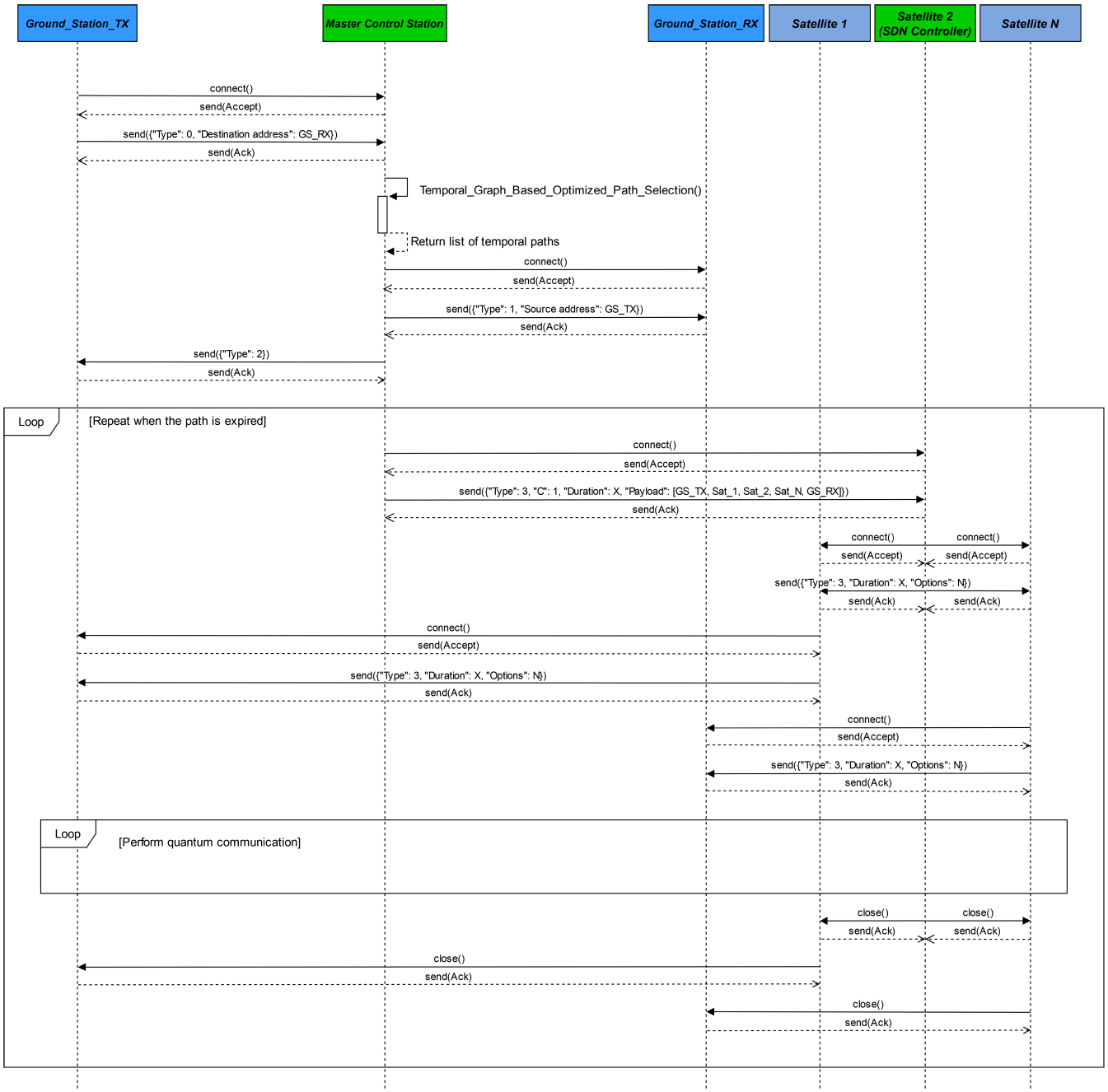

FIGURE 4. Sequence diagram for the proposed protocol. The quantum communication can occur once the E2E path is configured.

In parallel, the MCS sends a message with `T` configured as 1 to the destination GS to verify whether it can accept the connection. Whether the destination GS acknowledges the request, the MCS performs the placement of the SDN Controller in a favorable position of the path. This saves time in the setup of the path by operating simultaneously on the two sections into which it has been divided. Therefore, a connection is established with the satellite positioned in the middle of the path and a message with `T` configured as 3 message is sent with the `C` bit set to 1, which indicates that the satellite is designated as the SDN Controller.

Furthermore, the packet will also contain the duration field indicating the period of validity of the E2E path. This field is useful for the Controller to know how long it will need to schedule the other QSRs to operate. In this case, the `Extended` contains the addresses of the GSs and the QSRs that compose the path during the period specified in `Duration`.

At this time, the second phase starts and the Controller sends messages with `T` set to 3 to the QSRs that compose the path. The addresses are retrieved from the `Extended` of the previously received packet. Moreover, in the `Duration`

field of these messages is copied the value present in the `Duration` field of the message previously received from the MCS. The `Options` field can contain the number of qubits of the QMs related to the specific session half of which are associated with the `In interface label` and the other half with the `Out interface label`. These fields are associated with the logical interfaces depicted in Fig. 2. At this point, the configuration procedure is completed, and the quantum communication can be started.

Once the path is no longer available, the connections are closed, and the MCS will allocate a new path valid for the subsequent time interval repeating the procedure. The time required to establish a new path, in addition to depending on the protocol setup operations, is given by the time required to realign the optical pointer towards another satellite, which can be significant.

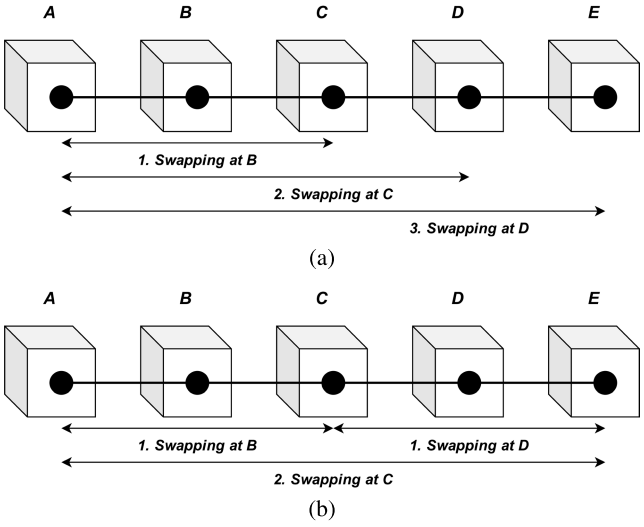

FIGURE 5. In a) is represented an entanglement swapping procedure on multiple devices performed from left to right. Fig. b) represents a procedure in which nodes B and D are swapped first. The procedure in b) can also be performed in reverse, starting from node C [47].

The system also provides for the possibility of choosing the entanglement generation procedure, several of which are represented in Fig. 5 in order to make the network as flexible as possible and adapt it to changing scenario conditions.

IV. PERFORMANCE EVALUATION

In this Section, we first characterize the adopted framework used for the modeling and testing of the proposed approach. All the trajectory data were obtained considering the Two-Line Element Set (TLEs) [48], which is a data format encoding a list of orbital parameters of Earth-orbiting objects for a specific point in time, the epoch. The TLEs allow rapid and extremely precise estimation of the movement of objects in orbit around Earth. The temporal graph of the satellite constellation is computed from the data obtained from these files obtained from [49] that allow

TABLE 1. Parameters and related values adopted in the performed simulations.

List of Parameters	Values
Wavelength	1550 nm [6]
Permittivity	1.000536 $\frac{C^2}{Nm^2}$ [51]
Conductivity	8×10^{-15} $\frac{S}{m}$ [52]
Optical BSM efficiency	0.75 [39], [40]
Atomic BSM efficiency	0.75 [41]
Optical BSM duration	10×10^{-6} s [10]
Atomic BSM duration	10×10^{-6} s [10]
Herald detector efficiency	0.95 [42]
Herald detector duration	10×10^{-6} s [10]
Telecom detector efficiency	0.8 [6]
Telecom detector duration	0.39×10^{-6} s [10]

to calculate the satellite trajectories. Specifically, we used the `Satellite Scenario Basic` of the `Satellite Communications Toolbox` Matlab package [50] in order to operate on the file containing the TLE coordinates to get the data related to the satellites' motions and the specific time intervals, which are necessary to create a temporal graph.

The simulations were performed by interconnecting two GSs on the surface of Earth placed at the antipodes considering the meeting point of the Greenwich meridian and the Equator. The considered scenario constitutes the worst case since the number of satellites visible to the GSs is as minimum as possible, and the distances between the GSs and the available satellites may be greater w.r.t. other coordinates. Furthermore, we calculated a temporal graph for a LEO constellation composed of 75 satellites based on data obtained by processing the TLE of the Iridium NEXT constellation for an overall time interval of 6 h with an accuracy of 1 s. We modeled the quantum system as in [6] and [7] considering the parameters specified in Table 1.

Fig. 6 shows the duration of time intervals when GSs are simultaneously in contact with the selected satellites. The results correspond to the path durations calculated by solving the optimization problem given in eq. (3). As can be seen from Fig. 6, the average value is about 276.9 s. It is important to find paths that have a duration corresponding to these time intervals, thereby limiting the connection set-up as few times as possible. Fig. 7 shows the length of the inter-satellite links obtained as a result of the optimization procedure, i.e., related to the best paths. Furthermore, Fig. 8 represents the total length of the path obtained on E2E basis with the considered procedure. The paths calculated in the time intervals resulting from the performed simulations always involve a number of satellites equal to 6, therefore the E2E paths are always composed of 7 links.

Finally, Fig. 9 shows the achievable entanglement rate on the E2E paths that have the duration and length characteristics

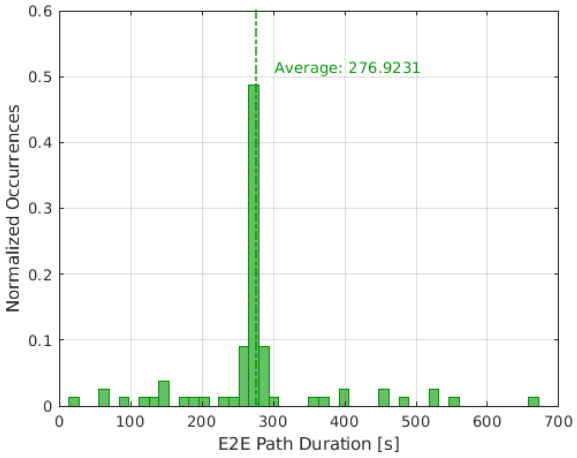

FIGURE 6. Duration of time intervals when GSs are simultaneously in contact with the optimal path.

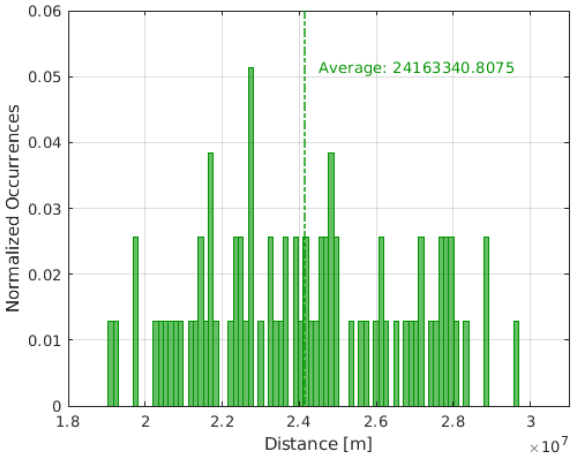

FIGURE 8. Total E2E path length.

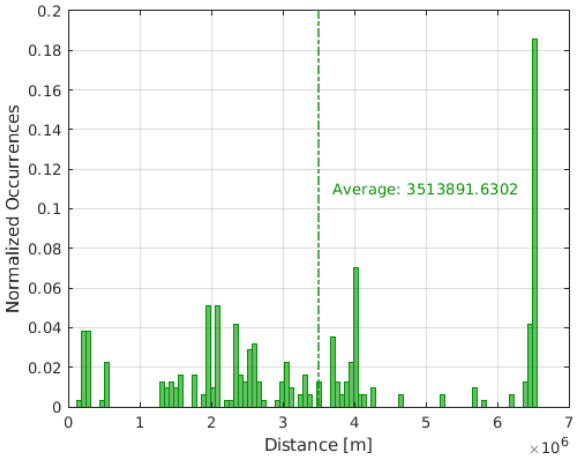

FIGURE 7. Inter-satellite distance between the satellites which constitute the E2E path.

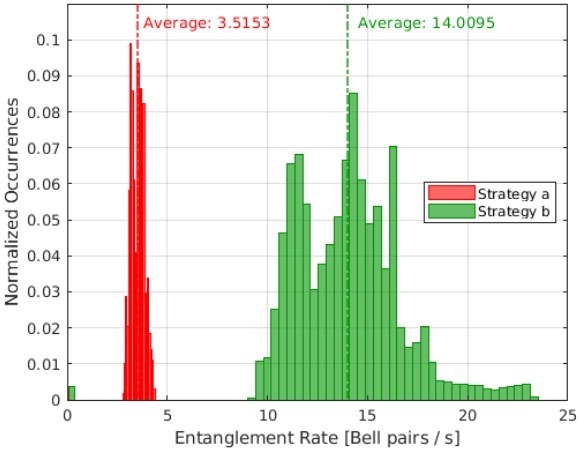

FIGURE 9. Entanglement rate calculated on the selected paths. The entanglement generation strategy represented in 5b ensures better performance.

described in Fig.s 6, 7, and 8, for the considered entanglement generation strategies. Specifically, the histogram in red is related to the strategy represented in Fig. 5a, while the green one is related to Fig. 5b, which ensures better performance. This is due to the fact that some of the devices that compose the path perform the operations in a synchronized manner, allowing saving time during the generation of pairs. Moreover, considering that, as specified previously, the number of satellites is always the same, the rate changes only as a function of distance, which affects the latency of the classical signal and therefore the probability of success in generating entanglement.

In Fig. 10, the performance in terms of entanglement rate of the best path that has the longest duration within a specific time interval and a sub-optimal path in terms of normalized occurrences is represented. As can be seen, the most durable E2E path, which is represented in green, is also the one that provides better performance. As a matter of fact, although it is possible to establish other paths during the time intervals constrained by the GSs, these are not durable and experience disconnection that severely degrades performance. As can be seen in Fig. 10, some values result equal to zero but only for the sub-optimal path that is not valid for the entire considered time interval.

Furthermore, Fig. 11 represents the value of the entanglement rate considering sessions of different durations. The results were obtained considering the strategy shown in Fig. 5b, and as can be seen, the average rate does not depend on the session duration. This is due to the fact that, during longer sessions, more path disconnections are likely to occur as well as additional paths characterized by better performance could be available.

Finally, in Fig. 12, is represented the cumulative number of Bell pairs generated during each of the 78 time intervals that occurs in the simulated scenario, which has a total duration of 6 h. As can be seen, the total number of generated Bell pairs has an average value close to 1000. Although the performance does not seem particularly remarkable,

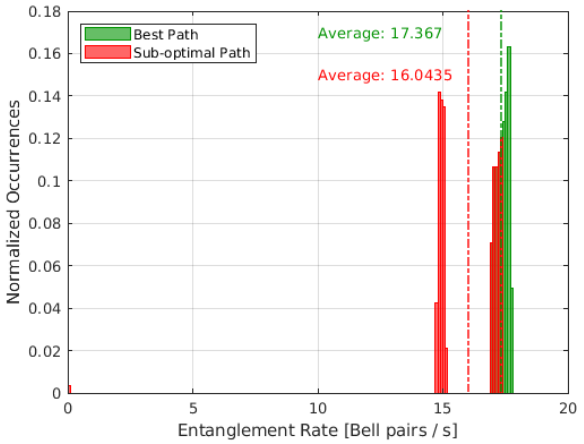

FIGURE 10. Performance of the best path that remains connected for the entire duration of one of the favorable time intervals w.r.t. a sub-optimal path.

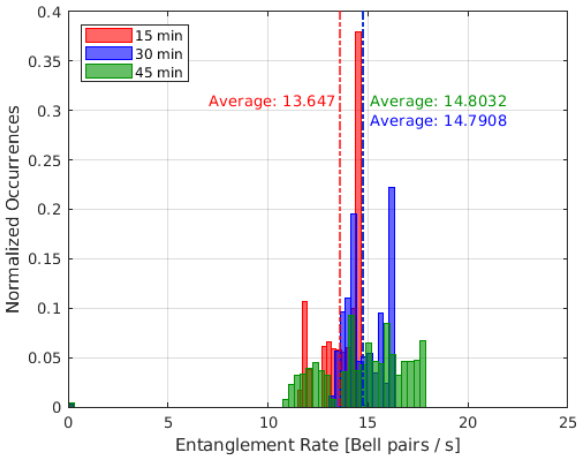

FIGURE 11. Entanglement rate considering sessions of different durations.

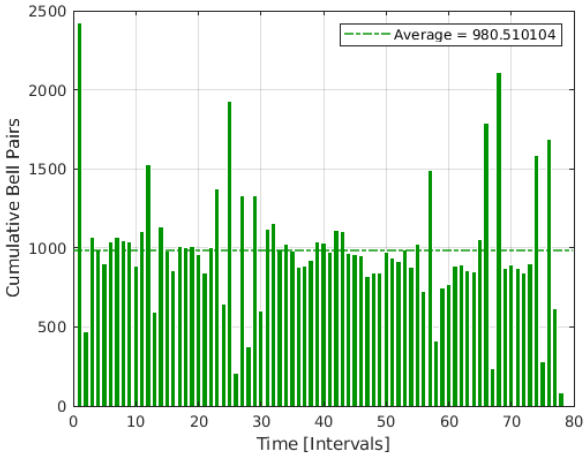

FIGURE 12. Cumulative Bell pairs generated during each time interval constrained by the GSs.

it is necessary to take into account that they are related to a worst case hypothesis that is the use of a single memory cell. Therefore, considering that multiple qubits of a single device could be dedicated to the same session, the network could ensure adequate performance to meet the requirements of different kinds of quantum applications.

V. CONCLUSION

Given the recent advances in the manufacturing of QDs, it is also extremely important to design specific networks based on the principles of quantum physics connecting quantum servers on Earth to realize Quantum Clouds to achieve an extraordinary computational capacity. Furthermore, there has been recently considerable interest in the development of specific quantum satellite networks, especially LEO. Although experiments have been conducted with single satellites, and an entire QR enabled LEO satellite constellation has not been launched yet.

The previous considerations motivated our investigation on the design of an efficient LEO quantum satellite backbone. Considering that the creation of distributed routing strategies and management protocols is difficult in the quantum case, the adoption of the SDN paradigm is considered crucial for quantum networking. Furthermore, satellites in LEO orbit move very rapidly and, therefore, this scenario can be studied with the theory of TNs. Hence, our paper provides a possible solution for the design of an SDN-based quantum satellite backbone control network with the conceptualization and performance evaluation of an innovative path selection algorithm, which can be applied to temporal graphs in order to limit the disconnections, also proposing a specifically designed protocol. Furthermore, we have applied specific entanglement generation methodologies trying to guarantee the highest possible performance of the future quantum constellations.

The system was studied considering a worst-case scenario in which two GSs located at the antipodes were connected. The results reveal that despite some technological limitations related to the capacity of QMs and their performance, the proposed architecture could support some types of quantum applications within the duration of each path and, therefore, without disconnection.

The issues that can arise with this kind of satellite networks equipped with QDs have to be explored further. In the future, the analysis can be extended by considering technological improvements related to the peculiarities of the QRs with which the satellites that will constitute these networks will be equipped. In addition, the study of quantum cloud systems to be integrated directly into satellite constellations for specific applications.

REFERENCES

[1] Y. Lu and X. Zheng, "6G: A survey on technologies, scenarios, challenges, and the related issues," *J. Ind. Inf. Integr.*, vol. 19, Sep. 2020, Art. no. 100158.

[2] M. M. Azari, S. Solanki, S. Chatzinotas, O. Kodheli, H. Sallouha, A. Colpaert, J. F. M. Montoya, S. Pollin, A. Haqiqatnejad, A. Mostaani, E. Lagunas, and B. Ottersten, "Evolution of non-terrestrial networks from 5G to 6G: A survey," *IEEE Commun. Surveys Tuts.*, vol. 24, no. 4, pp. 2633–2672, 4th Quart., 2022.

[3] I. F. Akyildiz, A. Kak, and S. Nie, "6G and beyond: The future of wireless communications systems," *IEEE Access*, vol. 8, pp. 133995–134030, 2020.
[4] M. Erhard, M. Krenn, and A. Zeilinger, "Advances in high-dimensional quantum entanglement," *Nature Rev. Phys.*, vol. 2, no. 7, pp. 365–381, Jun. 2020.
[5] C. H. Bennett, G. Brassard, C. Crépeau, R. Jozsa, A. Peres, and W. K. Wootters, "Teleporting an unknown quantum state via dual classical and einstein-podolsky-rosen channels," *Phys. Rev. Lett.*, vol. 70, no. 13, pp. 1895–1899, Mar. 1993.
[6] R. Picchi, F. Chiti, R. Fantacci, and L. Pierucci, "Towards quantum satellite internetworking: A software-defined networking perspective," *IEEE Access*, vol. 8, pp. 210370–210381, 2020.
[7] F. Chiti, R. Fantacci, R. Picchi, and L. Pierucci, "Quantum satellite backbone networks design and performance evaluation," in *Proc. ICC—IEEE Int. Conf. Commun.*, Jun. 2021, pp. 1–6.
[8] F. Chiti, R. Fantacci, R. Picchi, and L. Pierucci, "Towards the quantum Internet: Satellite control plane architectures and protocol design," *Future Internet*, vol. 13, no. 8, p. 196, Jul. 2021.
[9] D. Cuomo, M. Caleffi, and A. S. Cacciapuoti, "Towards a distributed quantum computing ecosystem," *IET Quantum Commun.*, vol. 1, no. 1, pp. 3–8, Jul. 2020, doi: 10.1049/iet-qtc.2020.0002.
[10] M. Caleffi, "Optimal routing for quantum networks," *IEEE Access*, vol. 5, pp. 22299–22312, 2017.
[11] L. Gyongyosi and S. Imre, "Entanglement access control for the quantum Internet," *Quantum Inf. Process.*, vol. 18, no. 4, p. 107, Feb. 2019.
[12] M. A. Nielsen and I. L. Chuang, *Quantum Computation and Quantum Information: 10th Anniversary Edition*. Cambridge, U.K.: Cambridge Univ. Press, 2010.
[13] G. Guccione, T. Darras, H. Le Jeannic, V. B. Verma, S. W. Nam, A. Cavaillès, and J. Laurat, "Connecting heterogeneous quantum networks by hybrid entanglement swapping," *Sci. Adv.*, vol. 6, no. 22, May 2020, Art. no. eaba4508, doi: 10.1126/sciadv.aba4508.
[14] Q. Ruihong and M. Ying, "Research progress of quantum repeaters," *J. Phys. Conf. Ser.*, vol. 1237, no. 5, Jun. 2019, Art. no. 052032.
[15] K. Hammerer, A. S. Sørensen, and E. S. Polzik, "Quantum interface between light and atomic ensembles," *Rev. Modern Phys.*, vol. 82, no. 2, pp. 1041–1093, Apr. 2010.
[16] L. Bacsardi, "On the way to quantum-based satellite communication," *IEEE Commun. Mag.*, vol. 51, no. 8, pp. 50–55, Aug. 2013.
[17] B.-C. Ciobanu, V. Iancu, and P. G. Popescu, "EntangleNetSat: A satellite-based entanglement resupply network," *IEEE Access*, vol. 10, pp. 69963–69971, 2022.
[18] A. Lalbakhsh, A. Pitcairn, K. Mandal, M. Alibakhshikenari, K. P. Esselle, and S. Reisenfeld, "Darkening low-Earth orbit satellite constellations: A review," *IEEE Access*, vol. 10, pp. 24383–24394, 2022.
[19] P. Holme and J. Saramäki, *Temporal Networks*. Cham, Switzerland: Springer, 2013.
[20] S. Brito, A. Canabarro, D. Cavalcanti, and R. Chaves, "Satellite-based photonic quantum networks are small-world," *PRX Quantum*, vol. 2, no. 1, Jan. 2021, Art. no. 010304.
[21] H. Wu, J. Cheng, S. Huang, Y. Ke, Y. Lu, and Y. Xu, "Path problems in temporal graphs," *Proc. VLDB Endowment*, vol. 7, no. 9, pp. 721–732, May 2014.
[22] W. Kozlowski and S. Wehner, "Towards large-scale quantum networks," in *Proc. 6th Annu. ACM Int. Conf. Nanosc. Comput. Commun.* New York, NY, USA: Association for Computing Machinery, Sep. 2019, pp. 1–7.
[23] H. Farhady, H. Lee, and A. Nakao, "Software-defined networking: A survey," *Comput. Netw.*, vol. 81, pp. 79–95, Apr. 2015.
[24] W. Jiang, "Software defined satellite networks: A survey," *Digit. Commun. Netw.*, vol. 9, no. 6, pp. 1243–1264, Dec. 2023.
[25] H.-Y. Liu, X.-H. Tian, C. Gu, P. Fan, X. Ni, R. Yang, J.-N. Zhang, M. Hu, J. Guo, X. Cao, X. Hu, G. Zhao, Y.-Q. Lu, Y.-X. Gong, Z. Xie, and S.-N. Zhu, "Optical-relayed entanglement distribution using drones as mobile nodes," *Phys. Rev. Lett.*, vol. 126, no. 2, Jan. 2021, Art. no. 020503.
[26] F. Chiti, R. Picchi, and L. Pierucci, "Metropolitan quantum-drone networking and computing: A software-defined perspective," *IEEE Access*, vol. 10, pp. 126062–126073, 2022.
[27] C. Liorni, H. Kampermann, and D. Bruß, "Quantum repeaters in space," *New J. Phys.*, vol. 23, no. 5, May 2021, Art. no. 053021.
[28] Y. Xue, "Satellite-relayed intercontinental quantum network," *J. Phys. Conf. Ser.*, vol. 2229, no. 1, Mar. 2022, Art. no. 012028.
[29] C.-Y. Lu, Y. Cao, C.-Z. Peng, and J.-W. Pan, "Micius quantum experiments in space," *Rev. Modern Phys.*, vol. 94, no. 3, Jul. 2022, Art. no. 035001.
[30] M. Gündoğan, J. S. Sidhu, V. Henderson, L. Mazzarella, J. Wolters, D. K. L. Oi, and M. Krutzik, "Proposal for space-borne quantum memories for global quantum networking," *npj Quantum Inf.*, vol. 7, no. 1, p. 128, Aug. 2021.
[31] J. Wallnöfer, F. Hahn, M. Gündoğan, J. S. Sidhu, F. Wiesner, N. Walk, J. Eisert, and J. Wolters, "Simulating quantum repeater strategies for multiple satellites," *Commun. Phys.*, vol. 5, no. 1, p. 169, Jun. 2022.
[32] C. Chen, Z. Liao, Y. Ju, C. He, K. Yu, and S. Wan, "Hierarchical domain-based multicontroller deployment strategy in SDN-enabled space–air–ground integrated network," *IEEE Trans. Aerosp. Electron. Syst.*, vol. 58, no. 6, pp. 4864–4879, Dec. 2022.
[33] J. Guo, L. Yang, D. Rincón, S. Sallent, Q. Chen, and X. Liu, "Static placement and dynamic assignment of SDN controllers in LEO satellite networks," *IEEE Trans. Netw. Service Manage.*, vol. 19, no. 4, pp. 4975–4988, Dec. 2022.
[34] L. de Forges de Parny, O. Alibart, J. Debaud, S. Gressani, A. Lagarrigue, A. Martin, A. Metrat, M. Schiavon, T. Troisi, E. Diamanti, P. Gélard, E. Kerstel, S. Tanzilli, and M. Van Den Bossche, "Satellite-based quantum information networks: Use cases, architecture, and roadmap," *Commun. Phys.*, vol. 6, no. 1, p. 12, Jan. 2023.
[35] F. Chiti, R. Fantacci, R. Picchi, and L. Pierucci, "Mobile control plane design for quantum satellite backbones," *IEEE Netw.*, vol. 36, no. 1, pp. 91–97, Jan. 2022.
[36] U. C. Guard, "Navstar gps user equipment introduction (public release version)," *Papers Published J. Navigat.*, vol. 1, pp. 5–6, Sep. 1996.
[37] A. Badie-Modiri, M. Karsai, and M. Kivelä, "Efficient limited-time reachability estimation in temporal networks," *Phys. Rev. E, Stat. Phys. Plasmas Fluids Relat. Interdiscip. Top.*, vol. 101, no. 5, May 2020, Art. no. 052303.
[38] T. Erlebach, M. Hoffmann, and F. Kammer, "On temporal graph exploration," *J. Comput. Syst. Sci.*, vol. 119, pp. 1–18, Aug. 2021.
[39] F. Ewert and P. van Loock, "3/4-efficient bell measurement with passive linear optics and unentangled ancillae," *Phys. Rev. Lett.*, vol. 113, no. 14, Sep. 2014, Art. no. 140403.
[40] W. P. Grice, "Arbitrarily complete bell-state measurement using only linear optical elements," *Phys. Rev. A*, vol. 84, no. 4, Oct. 2011, Art. no. 042331.
[41] S.-J. Yang, X.-J. Wang, X.-H. Bao, and J.-W. Pan, "An efficient quantum light–matter interface with sub-second lifetime," *Nature Photon.*, vol. 10, no. 6, pp. 381–384, Jun. 2016.
[42] S. Ramelow, A. Mech, M. Giustina, S. Gröblacher, W. Wieczorek, J. Beyer, A. Lita, B. Calkins, T. Gerrits, S. W. Nam, A. Zeilinger, and R. Ursin, "Highly efficient heralding of entangled single photons," *Opt. Exp.*, vol. 21, no. 6, p. 6707, Mar. 2013.
[43] W. Huo and V. J. Tsotras, "Efficient temporal shortest path queries on evolving social graphs," in *Proc. 26th Int. Conf. Sci. Stat. Database Manage.* New York, NY, USA: Association for Computing Machinery, Jun. 2014, pp. 1–4, doi: 10.1145/2618243.2618282.
[44] (2023). *Types of Orbits*. Accessed: Apr. 16, 2023. [Online]. Available: https://www.esa.int/Enabling_Support/Space_Transportation/Types_of_orbits
[45] J. Illiano, M. Caleffi, A. Manzalini, and A. S. Cacciapuoti, "Quantum Internet protocol stack: A comprehensive survey," *Comput. Netw.*, vol. 213, Aug. 2022, Art. no. 109092.
[46] A. A. Farid and S. Hranilovic, "Outage capacity optimization for free-space optical links with pointing errors," *J. Lightw. Technol.*, vol. 25, no. 7, pp. 1702–1710, Jul. 7, 2007.
[47] T. Matsuo, C. Durand, and R. Van Meter, "Quantum link bootstrapping using a ruleset-based communication protocol," *Phys. Rev. A*, vol. 100, no. 5, Nov. 2019, Art. no. 052320.
[48] D. A. Vallado and P. J. Cefola, "Two-line element sets-practice and use," in *Proc. 63rd Int. Astron. Congr. Naples, Italy*, 2012, pp. 1–14.

[49] *Norad Gp Element Sets Current Data*. Accessed: Apr. 19, 2023. [Online]. Available: https://celestrak.org/NORAD/elements/
[50] MathWorks Inc. (2022). *Satellite Communications Toolbox Version: 1.3 (R2022B)*. [Online]. Available: https://it.mathworks.com/products/satellite-communications.html
[51] (2010). *The Engineering Toolbox (2010). Relative Permittivity—The Dielectric Constant*. Accessed: Nov. 13, 2023. [Online]. Available: https://www.engineeringtoolbox.com/relative-permittivity-d_1660.html
[52] P. Helmenstine and A. Marie. (2023). *Table of Electrical Resistivity and Conductivity*. Accessed: Nov. 13, 2023. [Online]. Available: https://www.thoughtco.com/table-of-electrical-resistivity-conductivity-608499

FRANCESCO CHITI (Senior Member, IEEE) is currently an Associate Professor with the University of Florence. He is the author of six book chapters, more than 50 articles in international journals, and more than 70 conferences presentations. His research interests include ad-hoc networks and the software defined Internet of Things, has been conducted in several EU initiatives (COST 289, IP GoodFood, NoE NEWCOM, CRUISE NoE, STREP DustBot, REGPOT AgroSense, and EDA MEDUSA). He is serving as the Chair for IEEE Communications and Information Security Technical Committee and he has been the Co-Chair for the ''Communication & Information Systems Security'' Symposium at IEEE Globecom 2016. He is an Associate Editor of *International Journal on Security and Communication Networks* (Wiley), *Security and Privacy* (Wiley), and *Peer-to-Peer Networking and Applications* (Springer).

ROBERTO PICCHI (Member, IEEE) received the master's and Ph.D. degrees from the University of Florence. His research interests include quantum networking architecture and the foundation of the quantum internet to the Internet of Things and software-defined networking.

LAURA PIERUCCI (Senior Member, IEEE) received the Graduate degree in electronics engineering from the University of Florence, Florence, Italy, in 1987. She has been with the Department of Information Engineering, University of Florence, as an Assistant Professor, since 2000. She co-invented a patent on the use of RFID for health application. She has been involved in several national and European research projects on satellite communications, tele-medicine systems, wireless systems, and radar signal processing. She has been the Scientific Coordinator of the EU COST Action 252. She has served as an Expert for European Committee in the area of satellite communications. She has coauthored several international articles. Her current research interests include wireless communication systems especially in the topics of 4G/5G systems, resource management, D2D communications, multiple-input multiple-output antenna systems, cooperative communications, and security for wireless sensor networks and IoT. She was a recipient of the IWCMC 2016 Best Paper Award and the Globecom 2016 Best Paper Award. She is currently serving as an Associate Editor for *Telecommunication Systems*, *IEEE Communications Magazine*, and IEEE INTERNET OF THINGS JOURNAL.

Open Access funding provided by 'Università degli Studi di Firenze' within the CRUI CARE Agreement